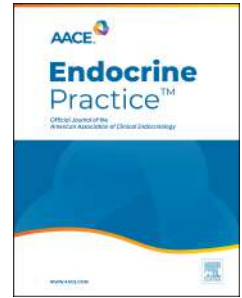


# Journal Pre-proof

Phosphatonins: From Discovery to Therapeutics

Kittrawee Kritmetapak, MD, Rajiv Kumar, MBBS, MACP



PII: S1530-891X(22)00625-5

DOI: <https://doi.org/10.1016/j.eprac.2022.09.007>

Reference: EPRAC 438

To appear in: *Endocrine Practice*

Received Date: 22 July 2022

Revised Date: 22 September 2022

Accepted Date: 23 September 2022

Please cite this article as: Kritmetapak K, Kumar R, Phosphatonins: From Discovery to Therapeutics, *Endocrine Practice* (2022), doi: <https://doi.org/10.1016/j.eprac.2022.09.007>.

This is a PDF file of an article that has undergone enhancements after acceptance, such as the addition of a cover page and metadata, and formatting for readability, but it is not yet the definitive version of record. This version will undergo additional copyediting, typesetting and review before it is published in its final form, but we are providing this version to give early visibility of the article. Please note that, during the production process, errors may be discovered which could affect the content, and all legal disclaimers that apply to the journal pertain.

© 2022 Published by Elsevier Inc. on behalf of the AACE.

**Phosphatonins: From Discovery to Therapeutics**

**Kittrawee Kritmetapak MD**, Faculty of Medicine Khon Kaen University, Khon Kaen, Thailand

**Rajiv Kumar MBBS, MACP**, Division of Nephrology and Hypertension, Mayo Clinic, Rochester, Minnesota, USA

**Corresponding author and contact information:** Rajiv Kumar MBBS, MACP, Division of Nephrology and Hypertension, Medical Sciences Building 1-120, Mayo Clinic, 200 1st St Southwest, Rochester, Minnesota 55905, USA

Telephone 507-284-9536

E-mail: [rkumar@mayo.edu](mailto:rkumar@mayo.edu)

**Sources of support:** NIH/NIDDK and the Frank B. and Kathryn C. Andersen Foundation. Dr. Kritmetapak was a visiting research fellow supported by a grant from Khon Kaen University.

**Short running title:** Phosphatonins

**Acknowledgements:** None

## 21 **Structured Abstract**

22 Phosphate is crucial for cell signaling, energy metabolism, nucleotide synthesis, and bone  
23 mineralization. The gut-bone-parathyroid-kidney axis is influenced by parathyroid hormone  
24 (PTH), 1,25-dihydroxyvitamin D (1,25(OH)<sub>2</sub>D), and phosphatonins, and facilitates maintenance  
25 of phosphate homeostasis. Phosphatonins including fibroblast growth factor 23 (FGF23),  
26 secreted frizzled-related protein 4 (sFRP4), matrix extracellular phosphoglycoprotein (MEPE),  
27 and fibroblast growth factor 7 (FGF7) play a pathogenic role in several hypophosphatemic  
28 disorders. Excess FGF23 inhibits sodium-dependent phosphate cotransporters (NaPi-2a and  
29 NaPi-2c), resulting in hyperphosphaturia and hypophosphatemia. Additionally, FGF23  
30 suppresses 1,25(OH)<sub>2</sub>D synthesis in the proximal renal tubule, and thus it indirectly inhibits  
31 intestinal phosphate absorption. Disorders of FGF23-related hypophosphatemia include X-linked  
32 hypophosphatemia (XLH), autosomal dominant hypophosphatemic rickets (ADHR), autosomal  
33 recessive hypophosphatemic rickets (ARHR), fibrous dysplasia/McCune-Albright syndrome, and  
34 tumor-induced osteomalacia (TIO). Complications of conventional therapy with oral phosphate  
35 and vitamin D analogs comprise gastrointestinal distress, hypercalcemia, nephrocalcinosis, and  
36 secondary/tertiary hyperparathyroidism. In both children and adults with XLH and TIO, the anti-  
37 FGF23 antibody burosumab exhibits a favorable safety profile and is associated with healing of  
38 rickets in affected children and improvement of osteomalacia in both children and adults. This  
39 review summarizes current knowledge regarding the phosphate homeostasis, phosphatonin  
40 pathophysiology, and clinical implications of FGF23-related hypophosphatemic disorders, with  
41 specific focus on burosumab treatment.

42

## 43 **Introduction**

44 Phosphate plays crucial roles in cell signaling, energy metabolism, membrane function, and  
45 nucleotide synthesis.<sup>1-3</sup> Additionally, phosphate is essential for biomineralization<sup>4</sup> and metabolic  
46 pathways including glycolysis, ammoniogenesis, and phosphorylation. Moreover, phosphate  
47 regulates oxygen-carrying capacity via the generation of 2,3-diphosphoglycerate in erythrocytes.  
48 Approximately 85% of phosphate in the body is present in bone and teeth, 14% exists in soft  
49 tissues, and 1% is present in extracellular fluids. In plasma, approximately 85% of phosphate is  
50 present as free forms ( $\text{HPO}_4^{2-}$  and  $\text{H}_2\text{PO}_4^-$ ), 10% is bound to proteins, and 5% is complexed with  
51 cations.<sup>2</sup> Serum phosphate concentrations are higher in children than in adults; the reference  
52 range is 4-7 mg/dL in children compared with 2.5-4.5 mg/dL in adults. Serum phosphate  
53 concentrations exhibit a biphasic circadian rhythm. Values are lowest in the morning, peak first  
54 in the late afternoon and peak again in the late evening. Since transcellular shifting of phosphate  
55 occurs under certain circumstances, serum phosphate concentrations may not reflect true  
56 phosphate stores. Serum phosphate concentrations are dependent on dietary intake and are  
57 regulated by parathyroid hormone (PTH), fibroblast growth factor 23 (FGF23), and 1,25-  
58 dihydroxyvitamin D ( $1,25(\text{OH})_2\text{D}$ ) through feedback mechanisms (Figure 1).<sup>2</sup>

## 59 **Intestinal Phosphate Absorption**

60 Dietary phosphate intake averages 1,000-1,500 mg per day. Approximately 60-80% of dietary  
61 phosphate is absorbed mostly through the proximal small intestine. Intestinal phosphate  
62 absorption occurs via two pathways: a passive paracellular and an active transcellular pathway  
63 (Figure 2).<sup>5,6</sup> Passive transport mechanisms depend on electrochemical phosphate gradients  
64 across the intestinal epithelial cell layer with paracellular movement mediated by tight junction

65 proteins. The active transcellular transport of phosphate is mediated by the sodium-phosphate  
66 cotransporter 2b (NaPi-2b) on the apical membrane of enterocytes.<sup>7</sup> In addition, PiT-1 and, to a  
67 lesser extent, PiT-2 transporters also contribute to transcellular intestinal phosphate absorption.<sup>8</sup>  
68 The deletion of NaPi-2b gene results in compensatory increases in the renal tubular phosphate  
69 reabsorption which help to normalize serum phosphate concentrations.<sup>9</sup> NaPi-2b expression is  
70 upregulated by the administration of 1,25(OH)<sub>2</sub>D and dietary phosphate restriction.<sup>6</sup> PTH  
71 indirectly induces changes in NaPi-2b expression through its stimulatory effect on renal  
72 1,25(OH)<sub>2</sub>D synthesis, which enhances NaPi-2b expression.<sup>10</sup>

### 73 **Renal Phosphate Transport**

74 The kidney is central to the regulation of phosphate homeostasis. Approximately 90-95% of  
75 circulating phosphate is filtered through the glomerulus, 80% of which is reabsorbed in the  
76 proximal tubule with less than 10% being reabsorbed in the distal nephron.<sup>2</sup> The renal tubular  
77 reabsorption of phosphate is mainly mediated by sodium-phosphate cotransporters (NaPi-2a,  
78 SLC34A1; NaPi-2c, SLC34A3; and PiT-2, SLC20A2) in the apical membrane of the proximal  
79 tubule (Figure 3).<sup>2</sup> The abundance of NaPi-2a and NaPi-2c is increased by low-phosphate diet  
80 and decreased by PTH.<sup>11</sup> PTH suppresses proximal tubular reabsorption of phosphate by  
81 internalizing NaPi-2a and NaPi-2c in the apical membrane through interaction with the scaffold  
82 protein Na<sup>+</sup>/H<sup>+</sup> exchanger regulatory factor 1 (NHERF1) and by increasing serine  
83 phosphorylation of NHERF1.<sup>12</sup> Additionally, dietary phosphate restriction induces apical  
84 membrane expression of PiT-2 in the proximal tubule.<sup>13</sup> Xenotropic and polytropic retrovirus  
85 receptor 1 (XPR1) could function as a basolateral phosphate transporter in the proximal tubule.<sup>14</sup>  
86 Mice with conditional inactivation of XPR1 gene in the renal tubule exhibit hypophosphatemic  
87 rickets and Fanconi syndrome with hyperphosphaturia.<sup>14</sup> Additional factors that increase renal

88 tubular phosphate reabsorption include volume contraction, metabolic alkalosis, 1,25(OH)<sub>2</sub>D,  
89 growth hormone, insulin, insulin-like growth factor 1, and thyroid hormone.<sup>2</sup> Conversely,  
90 additional factors that decrease renal tubular phosphate reabsorption include phosphate loading,  
91 volume expansion, metabolic acidosis, carbonic anhydrase inhibitors, calcitonin, atrial natriuretic  
92 peptide, dopamine, estrogen, and glucocorticoids.<sup>15-17</sup>

### 93 **Phosphatonins**

94 In 1994, the existence of phosphaturic factors (“phosphatonins”) that induce renal phosphate  
95 wasting in patients with tumor-induced osteomalacia (TIO) was described.<sup>18,19</sup> Conditioned  
96 medium from a tumor associated with TIO was found to secrete substances that inhibited  
97 sodium-dependent phosphate transport in opossum kidney epithelial cells. This heat-labile  
98 substance(s) inhibited phosphate transport via a cAMP-independent mechanism, and its action  
99 was not blocked by a PTH antagonist.<sup>18</sup> The phosphatonins have emerged as pivotal regulators of  
100 phosphate homeostasis which act by inducing a state of negative phosphate balance via direct  
101 inhibition of phosphate reabsorption in the proximal tubule and indirectly via the suppression of  
102 1,25(OH)<sub>2</sub>D production in the kidney. The currently known phosphatonins include fibroblast  
103 growth factor 23 (FGF23), matrix extracellular phosphoglycoprotein (MEPE), secreted frizzled-  
104 related protein 4 (sFRP4), and fibroblast growth factor 7 (FGF7).

### 105 **Fibroblast Growth Factor 23**

106 Fibroblast growth factor 23 (FGF23) is predominantly expressed in bone (osteocytes and  
107 osteoblasts). FGF23 is initially produced as a 251-amino acid prohormone which comprises three  
108 domains with the first 24 amino acids being the signal sequence, the middle portion of 155  
109 amino acids forming the core FGF homology domain, and the last 72 amino acids forming the C-

110 terminal domain of FGF23 (Figure 4).<sup>20</sup> After intracellular cleavage of the signal sequence,  
111 intact FGF23 (iFGF23) is O-glycosylated at threonine 178 by polypeptide N-  
112 acetylgalactosaminyltransferase 3 (GALNT3), which prevents proteolysis and facilitates the  
113 secretion of iFGF23 as a 227-amino acid glycoprotein with a molecular mass of 32 kDa and a  
114 plasma half-life of 45-60 minutes.<sup>21</sup> Alternatively, iFGF23 can be cleaved intracellularly by  
115 subtilisin-like proprotein convertases at the protease recognition site (R176XXR179), yielding  
116 biologically inactive N- and C-terminal FGF23 fragments that are cosecreted with iFGF23.<sup>22</sup> The  
117 balance between GALNT3-mediated O-linked glycosylation and proprotein convertase cleavage  
118 determines the amount of iFGF23 and FGF23 fragment in the circulation.<sup>23</sup>

119 The effects of FGF23 on phosphate homeostasis are mainly mediated by activation of the FGF  
120 receptor 1 (FGFR1) and require an alpha-klotho coreceptor that is highly expressed in the kidney  
121 and parathyroid gland.<sup>24</sup> The C-terminal domain of iFGF23 mediates binding of FGF23 to the  
122 FGFR-klotho complex.<sup>25</sup> C-terminal FGF23 fragments impair cellular signaling by competing  
123 with iFGF23 for binding to the FGFR-klotho complex.<sup>25</sup> FGF23 production in bone is stimulated  
124 by a variety of factors including high dietary or serum phosphate levels, PTH, 1,25(OH)<sub>2</sub>D,  
125 calcium, iron deficiency, erythropoietin, metabolic acidosis, and inflammatory cytokines.<sup>26</sup>

126 FGF23 reduces the expression of NaPi-2a and NaPi-2c transporters in the proximal tubule and  
127 increases phosphaturia.<sup>2</sup> Evidence shows that hypoparathyroid patients had higher serum  
128 phosphate and iFGF23 levels than healthy controls, but the fractional excretion of phosphate was  
129 comparable between the two groups.<sup>27</sup> This suggests that the existence of sufficient PTH might  
130 be necessary for the phosphaturic effect of FGF23. Further, serum calcium levels may also be  
131 involved in the modulation of FGF23 effects on renal tubular phosphate transport in patients with  
132 X-linked hypophosphatemia (XLH).<sup>28</sup> In the kidney, klotho is expressed mainly in the distal

133 tubule with lower abundance in the proximal tubule.<sup>29</sup> The circulating form of soluble klotho can  
134 also act as a coreceptor for FGF23 signaling. Moreover, klotho can act as a phosphaturic factor  
135 by diminishing the abundance of NaPi-2a in the proximal tubule.<sup>30</sup> FGF23 reduces serum  
136 1,25(OH)<sub>2</sub>D level by suppressing renal 1-alpha-hydroxylase (CYP27B1) expression and  
137 stimulating the 24-hydroxylase (CYP24A1) that converts 25(OH)D and 1,25(OH)<sub>2</sub>D into  
138 inactive metabolites.<sup>1</sup> Moreover, FGF23 directly suppresses PTH production from parathyroid  
139 glands through activation of both the klotho-dependent mitogen-activated protein kinase  
140 (MAPK) pathway and the klotho-independent calcineurin-mediated signaling pathway.<sup>31</sup> FGF23  
141 excess causes hypophosphatemia and reduced 1,25(OH)<sub>2</sub>D levels, whereas FGF23 deficiency  
142 causes hyperphosphatemia and elevated 1,25(OH)<sub>2</sub>D levels.<sup>22</sup>

#### 143 **Matrix Extracellular Phosphoglycoprotein**

144 Matrix extracellular phosphoglycoprotein (MEPE) is also among the most abundantly  
145 overexpressed genes found in TIO.<sup>32,33</sup> The intraperitoneal injection of MEPE causes  
146 hyperphosphaturia and hypophosphatemia in mice.<sup>34,35</sup> Additionally, MEPE inhibits phosphate  
147 uptake in human proximal tubular epithelial cells in vitro. Moreover, MEPE inhibits bone  
148 mineralization in vitro and MEPE null mice have increased bone mineralization.<sup>35</sup> These suggest  
149 that MEPE may play a role in the pathogenesis of XLH in which there is renal phosphate wasting  
150 and evidence for a mineralization defect that is independent of serum phosphate concentrations.  
151 Serum MEPE levels are elevated in patients with XLH.<sup>34</sup> PHEX prevents proteolysis of MEPE  
152 and release of an acidic serine aspartate-rich MEPE-associated motif (ASARM) peptide, an  
153 inhibitor of bone mineralization (minhibin).<sup>36</sup> PHEX and MEPE form a nonproteolytic protein  
154 interaction via the MEPE C-terminal ASARM motif. Inactivating mutations of PHEX increases  
155 the production of MEPE-derived ASARM peptide and may cause hypomineralization in XLH. A



156 subsequent study challenges this conclusion by demonstrating that the selective knockout of  
157 PHEX in osteoblasts of normal mice results in a disorder with bone abnormalities and decreased  
158 renal phosphate transport, similar to that in the Hyp-mouse, a murine model for XLH in humans.  
159 However, in this knockout animal model the serum levels of MEPE are normal, while these  
160 variables are elevated in Hyp-mice. These data indicate that MEPE may not participate in the  
161 pathophysiology of renal phosphate transport defect and possibly the bone mineralization  
162 abnormality in XLH.<sup>37</sup>

#### 163 **Secreted Frizzled-Related Protein 4**

164 Secreted frizzled-related protein 4 (sFRP4) is among the most consistently overexpressed genes  
165 found associated with TIO.<sup>32</sup> We have demonstrated that sFRP4 inhibited sodium-dependent  
166 phosphate transport by reducing NaPi-2a abundance in the brush border membrane of the  
167 proximal tubule and on the surface of opossum kidney epithelial cells.<sup>38</sup> Additionally, the  
168 intravenous infusion of sFRP4 increased phosphaturia, decreased serum phosphate, but did not  
169 alter renal 1-alpha-hydroxylase mRNA concentrations in rats. However, the expected increase in  
170 serum 1,25(OH)<sub>2</sub>D did not occur. Thus, sFRP4 may inhibit the compensatory upregulation of 1-  
171 alpha-hydroxylase activity and 1,25(OH)<sub>2</sub>D synthesis. The phosphaturic effects of sFRP4 were  
172 also demonstrated in thyroparathyroidectomized rats, suggesting the PTH-independent activity of  
173 sFRP4.<sup>39</sup> Genetic deletion of the sFRP4 gene in mice does not significantly impact serum or  
174 urine phosphate levels. Further, sFRP4 is unable to compensate for the absence of FGF23 or  
175 klotho since double knockouts have similar phenotypes as mice with deletion of FGF23 or klotho  
176 alone.<sup>40</sup> Furthermore, we observed that serum sFRP4 levels did not change with creatinine  
177 clearance or hyperphosphatemia in patients with CKD, and no correlation was found between  
178 post-kidney transplant serum sFRP4 levels and hypophosphatemia.<sup>41</sup> We created mice with a

179 global *Phex* knockout (*Cre-PhexDeltaflox/y* mice) and conditional osteocalcin (OC)-promoted  
180 *Phex* inactivation in osteoblasts and osteocytes (*OC-Cre-PhexDeltaflox/y*). Serum phosphate  
181 levels in *Cre-PhexDeltaflox/y*, *OC-Cre-PhexDeltaflox/y*, and *hyp*-mice were lower than those in  
182 normal mice. Kidney cell membrane phosphate transport in *Cre-PhexDeltaflox/y*, *OC-Cre-*  
183 *PhexDeltaflox/y*, and *hyp*-mice was likewise reduced compared with that in normal mice.  
184 Abnormal renal phosphate transport in *Cre-PhexDeltaflox/y* and *OC-Cre-PhexDeltaflox/y* mice  
185 was associated with increased bone production and serum FGF23 levels and decreased renal  
186 NaPi-2a protein, as was the case in *hyp*-mice. Additionally, *Cre-PhexDeltaflox/y*, *OC-Cre-*  
187 *PhexDeltaflox/y*, and *hyp*-mice manifested comparable osteomalacia. Serum FGF23, MEPE, and  
188 sFRP4 levels were increased in *hyp*- and *Cre-Phex<sup>Δflox/y</sup>* mice. However, serum FGF23, but not  
189 MEPE or sFRP4, was increased in *OC-Cre-Phex<sup>Δflox/y</sup>* mice.<sup>37</sup> Altogether, although sFRP4  
190 acutely alters renal phosphate handling and possibly 1,25(OH)<sub>2</sub>D physiology, most data  
191 demonstrate that it plays a minor role in the regulation of phosphate homeostasis.

## 192 **Fibroblast Growth Factor 7**

193 Previous research has shown that FGF7 is overexpressed in tumors associated with TIO.<sup>42</sup> FGF7  
194 inhibits sodium-dependent phosphate transport in opossum kidney epithelial cells and enhances  
195 phosphaturia in rats.<sup>43</sup> Moreover, circulating FGF7 levels are elevated in some patients with  
196 TIO.<sup>44</sup> A recent study showed that low serum FGF7 levels were observed in pediatric patients  
197 with hypophosphatasia and hyperphosphatemia.<sup>43</sup>

## 198 **FGF23-Related Hypophosphatemic Disorders**

### 199 **X-Linked Hypophosphatemia**

200 X-linked hypophosphatemia (XLH) is the most common inherited form of rickets with an  
201 estimated prevalence of 1 case per 20,000 live births.<sup>45,46</sup> XLH is an X-linked dominant disorder  
202 characterized by rickets and osteomalacia in children and osteomalacia in adults. The clinical  
203 manifestations of XLH are variable, ranging from isolated hypophosphatemia to severe bone  
204 disease. XLH generally manifests in the first one to two years of age when rickets and lower-  
205 extremity bowing become apparent with the onset of weight bearing.<sup>46,47</sup> Rickets also lead to  
206 short stature and growth retardation. The complications that occur more commonly in adults with  
207 XLH include osteomalacia with pseudofractures, chronic bone and joint pain, dental abscesses,  
208 enthesopathy (calcification of the tendons and ligaments in close proximity to bone),  
209 osteoarthritis, muscle weakness, and sensorineural hearing loss.<sup>1,46,47</sup> Laboratory findings show  
210 hypophosphatemia, hyperphosphaturia, normocalcemia, low or inappropriately normal serum  
211 1,25(OH)<sub>2</sub>D, and elevated serum alkaline phosphatase and FGF23 levels. FGF23-mediated  
212 1,25(OH)<sub>2</sub>D deficiency and oral phosphate therapy may lead to elevated PTH levels.<sup>47</sup>

213 PHEX (phosphate-regulating gene with homologies to endopeptidases on the X chromosome), a  
214 member of the M13 family of membrane-bound metalloproteases, has been identified as the gene  
215 inactivated in XLH.<sup>1</sup> PHEX is expressed predominantly in osteoblasts and osteocytes in bone,  
216 and odontoblasts in teeth.<sup>46</sup> PHEX is not responsible for direct proteolytic cleavage of FGF23.  
217 Instead, PHEX may activate the subtilisin-like proprotein convertase activity by promoting the  
218 transcription of its 7B2 chaperone protein.<sup>48</sup> Therefore, inactivating mutations of PHEX lead to  
219 reduced levels of 7B2 chaperone protein, diminished activity of subtilisin-like proprotein  
220 convertase, reduced FGF23 degradation, and increased serum levels of FGF23.<sup>48</sup> However, the  
221 mechanism by which PHEX mutation causes downregulation of 7B2 chaperone protein  
222 expression remains unknown. In addition to FGF23-mediated renal phosphate wasting, the

223 pathophysiology of XLH may involve the abnormal metabolism of PHEX substrates called small  
224 integrin-binding ligand N-linked glycoproteins (SIBLING), which include osteopontin, bone  
225 sialoprotein, dentin matrix protein 1, dentin sialophosphoprotein, and MEPE.<sup>49</sup> Therefore, PHEX  
226 deficiency in XLH patients causes the accumulation of SIBLING proteins and their fragments,  
227 which contribute to local inhibition of mineralization. Hypophosphatemia inhibits mineralization  
228 and leads to rickets by impairing caspase-mediated apoptosis of hypertrophic chondrocytes.<sup>50</sup>  
229 Furthermore, hypophosphatemia-independent effects of excessive FGF23 in bone including local  
230 inhibition of 1,25(OH)<sub>2</sub>D production and downregulation of tissue-nonspecific alkaline  
231 phosphatase also play a role in mineralization defect in XLH.<sup>51</sup> 1,25(OH)<sub>2</sub>D stimulates osteoblast  
232 differentiation and induces the generation of mature matrix vesicles, thereby facilitating  
233 mineralization process.<sup>52</sup>

#### 234 **Autosomal Dominant Hypophosphatemic Rickets**

235 Autosomal dominant hypophosphatemic rickets (ADHR) is a rare hereditary renal phosphate  
236 wasting disorder with phenotypes similar to XLH. The prevalence of ADHR is less than 1 cases  
237 per 100,000 live births. Approximately one-half of patients with ADHR present clinically  
238 evident disease, including rickets, at one to three years of age. In some affected children,  
239 hypophosphatemia persists into adulthood or remits after puberty. The remaining patients have  
240 delayed disease onset, ranging from 14 to 45 years. Late-onset ADHR may present with bone  
241 pain and hypophosphatemia in adulthood, but no lower-extremity deformities.<sup>46,49,53</sup> ADHR is  
242 caused by the mutation disrupting the R176XXR179 protease recognition site in FGF23, and the  
243 resultant mutant FGF23 is elevated due to reduced FGF23 cleavage.<sup>46</sup> Serum FGF23 levels  
244 usually fluctuate and reflect the disease activity of ADHR, partly depending on iron status.<sup>54,55</sup>  
245 Iron deficiency upregulates FGF23 expression in bone, and in normal individuals, intracellular

246 proteolysis of iFGF23 is efficient, thereby normalizing serum iFGF23 levels. However,  
247 inefficient degradation of mutant iFGF23 fails to compensate for increased FGF23 production  
248 during iron deficiency, thereby triggering ADHR symptoms. Thus, women with ADHR are at  
249 greater risk of developing hypophosphatemia during menstruation or pregnancy and correcting  
250 iron deficiency may improve symptoms.<sup>56</sup> Notably, certain intravenous iron preparations,  
251 especially ferric carboxymaltose (FCM), can increase serum FGF23 levels presumably by  
252 preventing cleavage of FGF23, thereby potentially exacerbating ADHR symptoms.<sup>57</sup> Several  
253 studies have reported that FCM resulted in high incidence of hypophosphatemia (serum  
254 phosphate <2.0 mg/dL), with values ranging from 64.0% to 75.0%, among patients with iron-  
255 deficiency anemia and normal kidney function.<sup>58,59</sup> Hypophosphatemia developed within 1 week  
256 of FCM administration, peaked in prevalence by week 2, and persisted through the end of the 5-  
257 week study. Reductions in serum phosphate were associated with contemporaneous increases in  
258 serum iFGF23, PTH, and FEPO<sub>4</sub>, and decreases in 1,25(OH)<sub>2</sub>D.<sup>58,59</sup>

### 259 **Autosomal Recessive Hypophosphatemic Rickets**

260 Autosomal recessive hypophosphatemic rickets (ARHR) is caused by inactivating mutations in  
261 the gene encoding dentin matrix protein 1 (DMP1), ectonucleotide  
262 pyrophosphatase/phosphodiesterase 1 (ENPP1), or the family with sequence similarity 20,  
263 member C (FAM20C).<sup>46</sup> DMP1 belongs to the large SIBLING family of extracellular matrix  
264 proteins and is mainly coexpressed with FGF23 in bone. ENPP1 is the transmembrane enzyme  
265 critical for the generation of inorganic pyrophosphate which is the mineralization inhibitor.<sup>60</sup>  
266 FAM20C directly phosphorylates FGF23 on serine 180, which inhibits GALNT3-mediated O-  
267 linked glycosylation, thus increasing intracellular FGF23 cleavage and reducing iFGF23  
268 secretion. The clinical manifestations of ARHR are similar to those of XLH and ADHR. Serum

269 FGF23 levels are elevated or high normal. Moreover, ENPP1 mutations are associated with  
270 generalized arterial calcification in infancy.<sup>61</sup> The mechanism by which inactivating mutations in  
271 DMP1 or ENPP1 increase FGF23 levels remains unclear.

### 272 **Fibrous Dysplasia/McCune-Albright Syndrome**

273 Fibrous dysplasia (FD) is a lesion in which portions of the bone are replaced by fibrous  
274 connective tissue and poorly formed trabecular bone. It is caused by somatic activating missense  
275 mutation of the guanine nucleotide stimulatory protein (GNAS1) gene that affects bone, skin,  
276 and endocrine system function.<sup>62,63</sup> The bones commonly affected by FD are proximal femur,  
277 tibia, ribs, and skull. FD may occur in single or multiple bones (monostotic and polyostotic  
278 fibrous dysplasia, respectively). McCune-Albright syndrome is characterized by polyostotic FD,  
279 café-au-lait macules and a variety of endocrine disorders, including precocious puberty, growth  
280 hormone hypersecretion, and hyperthyroidism.<sup>64</sup> Hypophosphatemia due to hyperphosphaturia is  
281 observed in approximately 50% of patients with FD/McCune-Albright syndrome and is  
282 associated with rickets or osteomalacia. Serum FGF23 levels are elevated due to a mass of  
283 FGF23-producing cells in fibrous bone lesions.<sup>65</sup>

### 284 **Tumor-Induced Osteomalacia (Oncogenic Osteomalacia)**

285 Tumor-induced osteomalacia (TIO) is a rare paraneoplastic syndrome induced by tumoral  
286 oversecretion of phosphaturic factors. The tumors frequently associated with TIO are  
287 phosphaturic mesenchymal tumors of mixed connective tissue type.<sup>66,67</sup> Additionally, TIO has  
288 been reported in patients with other malignancies, including colon, ovaries, prostate, and  
289 lymphoma.<sup>68</sup> These tumors typically secrete FGF23 and other phosphaturic proteins, including  
290 sFRP4, MEPE, and FGF7.<sup>1,33</sup> Elevated serum FGF23 levels were observed in 19 of 22 patients

291 with TIO (sensitivity, 86%).<sup>69</sup> TIO is more common in adults than children.<sup>70</sup> Clinical  
292 manifestations include muscle weakness, bone pain, fracture, osteomalacia, impaired bone  
293 microarchitecture,<sup>71-73</sup> normocalcemia, hypophosphatemia, hyperphosphaturia, elevated alkaline  
294 phosphatase, low or inappropriately normal 1,25(OH)<sub>2</sub>D levels, and normal or elevated PTH.  
295 Diagnosis of TIO depends on localization of the underlying tumor, which is usually small and in  
296 obscure location (e.g., lower extremities and head and neck regions).<sup>74</sup> Several techniques have  
297 been used to identify tumors responsible for TIO, including whole-body magnetic resonance  
298 imaging or sestamibi scan, somatostatin receptor scintigraphy, and somatostatin receptor positron  
299 emission tomography/computed tomography.<sup>75</sup> Systemic venous sampling for FGF23 is useful to  
300 determine whether an identified mass is secreting FGF23.<sup>76</sup> Complete tumor resection leads to an  
301 improvement of biochemical abnormalities and bone diseases.

## 302 **Evaluation of Hypophosphatemia**

303 The etiology of hypophosphatemia is often evident from the clinical history. If the diagnosis is  
304 uncertain, then evaluation of the fractional excretion of filtered phosphate (FEPO<sub>4</sub>) or tubular  
305 maximum reabsorption of phosphate per glomerular filtration rate (TmP/GFR) should be helpful.  
306 The FEPO<sub>4</sub> (phosphate/creatinine clearance ratio) is calculated using the formula: FEPO<sub>4</sub> =  
307 [urine phosphate (mg/dL) x serum creatinine (mg/dL)] / [serum phosphate (mg/dL) x urine  
308 creatinine (mg/dL)]. The fractional tubular reabsorption of phosphate (TRP) is calculated using  
309 the formula: TRP = 1 – FEPO<sub>4</sub>. The nomogram is entered with serum phosphate level and the  
310 TRP value, and the intersection of a straight line joining these values with the TmP/GFR scale is  
311 read (Figure 5).<sup>77</sup> The normal range for TmP/GFR in adults is 2.5-4.2 mg/dL; it is higher in  
312 children. A FEPO<sub>4</sub> of less than 20%, or a high TmP/GFR, indicates appropriate low urine  
313 phosphate excretion, suggesting that hypophosphatemia is caused by inadequate intake,

314 transcellular phosphate shift (e.g., respiratory alkalosis, refeeding syndrome), or decreased  
315 intestinal phosphate absorption (e.g., chronic diarrhea, malabsorption). Conversely, a FEPO<sub>4</sub> of  
316 greater than 20%, or a low TmP/GFR indicates renal phosphate wasting, suggesting that  
317 hypophosphatemia is caused by primary or secondary hyperparathyroidism, vitamin D  
318 resistance, FGF23-dependent hypophosphatemia, or renal tubular defects (Table 1). Euglycemic  
319 glycosuria, amino aciduria, tubular proteinuria, hyperuricosuria, and proximal renal tubular  
320 acidosis indicate a proximal tubular disorder, such as Fanconi syndrome. The measurement of  
321 serum PTH, 25(OH)D, 1,25(OH)<sub>2</sub>D, and serum FGF23 levels are necessary to determine the  
322 causes of hypophosphatemia secondary to renal phosphate losses. Hypophosphatemia due to  
323 hyperparathyroidism is generally less severe than FGF23-mediated hypophosphatemia because  
324 the serum levels of 1,25(OH)<sub>2</sub>D are higher. High serum FGF23, low serum 1,25(OH)<sub>2</sub>D, and  
325 adequate serum 25(OH)D should raise suspicion of FGF23-mediated hypophosphatemia,  
326 including XLH, ADHR, ARHR, FD, and TIO. The underlying mechanisms responsible for the  
327 increase in FGF23 are shown in Table 2. Although vitamin D deficiency and FGF23-mediated  
328 hypophosphatemic disorders sometimes coexist, serum FGF23 levels are elevated in the latter  
329 condition.

### 330 **Measurement of Circulating FGF23**

331 Currently, FGF23 immunoassays are mainly for research use. FGF23 immunoassays can either  
332 detect the intact form (iFGF23 immunoassay) or both the intact form and C-terminal fragments  
333 (cFGF23 immunoassay) that result from intracellular cleavage (Figure 6). Besides different  
334 reported units [iFGF23 in picograms per milliliter (pg/mL) and cFGF23 in relative units per  
335 milliliter (RU/mL)], absolute values between the assays vary widely due to different calibration,  
336 and no harmonization has been conducted.<sup>78,79</sup> Patients with XLH or TIO usually have serum



337 iFGF23 level (Kainos assay) above 30 pg/mL.<sup>80</sup> FGF23 is more stable in EDTA plasma than in  
338 serum at room temperature. Thus, FGF23 values obtained in EDTA plasma are higher than those  
339 obtained in serum. Whether plasma or serum should be used for FGF23 measurement is assay-  
340 specific. Previous studies have suggested that iFGF23 immunoassays are more sensitive than  
341 cFGF23 immunoassays for the measurement of circulating FGF23 concentrations in patients  
342 with TIO and patients with XLH. Additionally, iFGF23 concentrations are not affected by iron  
343 deficiency which may lead to false positive results when using cFGF23 immunoassays. Ideally,  
344 FGF23 should be measured 1 to 2 weeks after discontinuation of phosphate and 1,25(OH)<sub>2</sub>D  
345 since both agents may increase FGF23 levels.<sup>47</sup> Burosumab therapy may cause analytical  
346 interference with certain FGF23 immunoassays.<sup>81</sup>

### 347 **Management of FGF23-Related Hypophosphatemic Disorders**

348 Conventional treatment of XLH and TIO comprises oral phosphate and vitamin D analogs.  
349 Adverse effects of conventional treatment include gastrointestinal discomfort, hypercalciuria,  
350 nephrocalcinosis, and secondary/tertiary hyperparathyroidism due to chronic stimulation of  
351 parathyroid glands by oral phosphate. Moreover, conventional treatment increases FGF23 levels,  
352 potentially aggravating hypophosphatemia and 1,25(OH)<sub>2</sub>D deficiency. Thus, a reasonable  
353 approach is to use burosumab which is a human monoclonal antibody targeted to inhibit excess  
354 FGF23 bioactivity. Burosumab is administered subcutaneously, every 2 weeks (for children) or  
355 every 4 weeks (for adults) and has demonstrated efficacy with an acceptable safety profile in  
356 both pediatric and adult XLH cohorts. Oral phosphate and vitamin D analogs should be  
357 discontinued one week before initiating burosumab. Burosumab is contraindicated in patients  
358 with creatinine clearance below 30 mL/min. The common side effect of burosumab is a transient  
359 injection-site reaction.

360 The superiority of burosumab over conventional treatment in children with XLH has been  
361 demonstrated in terms of serum phosphate normalization, improvements in mineralization  
362 defects and lower-extremity deformities, improved physical ability, and reduced pain and the  
363 severity of rickets.<sup>82-86</sup> In a double-blind, placebo-controlled, phase 3 study in 134 adults with  
364 XLH, burosumab treatment for 24 weeks was associated with improvements in phosphate and  
365 vitamin D metabolism, enhanced fracture healing, and reduced stiffness.<sup>87</sup> After 24 weeks, all  
366 patients received open-label burosumab until week 48.<sup>88</sup> Burosumab treatment from weeks 24-48  
367 showed that serum phosphate remained normal in 83.8% of subjects who received burosumab  
368 throughout and were normalized in 89.4% who received burosumab after placebo. By week 48,  
369 63.1% of baseline fractures/pseudofractures healed completely with burosumab, compared with  
370 35.2% with burosumab after placebo. In both groups, burosumab was associated with clinically  
371 significant and sustained improvement from baseline to week 48 regarding stiffness, pain,  
372 physical function, and 6-min walk distance. Statistically significant improvements from baseline  
373 in patient-reported outcomes and ambulatory function persisted up to week 96 with burosumab  
374 treatment, with predefined meaningful changes observed in pain, stiffness, and fatigue.<sup>89</sup> Rates of  
375 adverse events were similar for burosumab and placebo. Furthermore, recent research has shown  
376 that adults with XLH who received burosumab had a significantly improvement in  
377 histomorphometric features of osteomalacia.<sup>90</sup>

378 Burosumab can also improve biochemical and bone abnormalities in patients with TIO. In an  
379 open-label, single-arm, phase 2 study, burosumab treatment of 14 adult patients with TIO up to  
380 144 weeks resulted in improvements in serum phosphate levels and bone histomorphometric  
381 measures of osteomalacia, enhanced fracture/pseudofracture healing, reductions in  
382 musculoskeletal pain, and improvement in functional mobility.<sup>91</sup> Burosumab exhibited an

383 acceptable safety profile. Main clinical studies of burosumab in adults with XLH or TIO are  
384 summarized in Table 3. Based on these results, burosumab has been approved for the treatment  
385 of XLH and TIO in both pediatric and adult patients in several countries including USA.  
386 Nevertheless, the current data does not indicate that burosumab treatment results in a complete  
387 normalization of osteomalacic disorders. This might be due to delayed treatment initiation or  
388 effects of non-FGF23 phosphatonins (FGF7, MEPE, and sFRP4) which are not blocked by  
389 burosumab. The use of burosumab in TIO should be limited to patients with unresectable tumors.  
390 Long-term efficacy and safety of burosumab on bone histomorphometry, kidney function, and  
391 vascular calcification deserve further studies.

## 392 **Conclusion**

393 Phosphatonins play an important role in phosphate homeostasis and bone mineralization. FGF23  
394 excess is central to the pathogenesis of most hypophosphatemic rickets and TIO. In adults and  
395 children with XLH and with TIO, the anti-FGF23 antibody burosumab significantly improves  
396 phosphate homeostasis, skeletal abnormalities, and quality of life and exhibits an acceptable  
397 safety profile. Whether blocking antibodies to other phosphatonins confer a benefit on certain  
398 patient subgroups with XLH or TIO requires further research.

399

## 400 **References**

- 401 1. Berndt T, Kumar R. Phosphatonins and the regulation of phosphate homeostasis. *Annu*  
402 *Rev Physiol* 2007;69:341-59.
- 403 2. Kritmetapak K, Kumar R. Phosphate as a Signaling Molecule. *Calcif Tissue Int*  
404 2021;108:16-31.
- 405 3. Michigami T, Kawai M, Yamazaki M, Ozono K. Phosphate as a Signaling Molecule and  
406 Its Sensing Mechanism. *Physiol Rev* 2018;98:2317-48.

- 407 4. Bhadada SK, Rao SD. Role of Phosphate in Biomineralization. *Calcif Tissue Int*  
408 2021;108:32-40.
- 409 5. Kritmetapak K, Kumar R. Novel Insights into Mechanisms of Intestinal Phosphate  
410 Absorption in Patients with Chronic Kidney Disease. *J Am Soc Nephrol* 2021;32:1830-2.
- 411 6. Hernando N, Gagnon K, Lederer E. Phosphate Transport in Epithelial and Nonepithelial  
412 Tissue. *Physiol Rev* 2021;101:1-35.
- 413 7. Marks J. The role of SLC34A2 in intestinal phosphate absorption and phosphate  
414 homeostasis. *Pflugers Arch* 2019;471:165-73.
- 415 8. Ichida Y, Ohtomo S, Yamamoto T, et al. Evidence of an intestinal phosphate transporter  
416 alternative to type IIb sodium-dependent phosphate transporter in rats with chronic kidney  
417 disease. *Nephrol Dial Transplant* 2021;36:68-75.
- 418 9. Lederer E, Miyamoto K. Clinical consequences of mutations in sodium phosphate  
419 cotransporters. *Clin J Am Soc Nephrol* 2012;7:1179-87.
- 420 10. Jacquillet G, Unwin RJ. Physiological regulation of phosphate by vitamin D, parathyroid  
421 hormone (PTH) and phosphate (Pi). *Pflugers Arch* 2019;471:83-98.
- 422 11. Lotscher M, Kaissling B, Biber J, Murer H, Levi M. Role of microtubules in the rapid  
423 regulation of renal phosphate transport in response to acute alterations in dietary phosphate  
424 content. *J Clin Invest* 1997;99:1302-12.
- 425 12. Weinman EJ, Steplock D, Shenolikar S, Blanpied TA. Dynamics of PTH-induced  
426 disassembly of Npt2a/NHERF-1 complexes in living OK cells. *Am J Physiol Renal Physiol*  
427 2011;300:F231-5.
- 428 13. Moe OW. PiT-2 coming out of the pits. *Am J Physiol Renal Physiol* 2009;296:F689-90.
- 429 14. Ansermet C, Moor MB, Centeno G, et al. Renal Fanconi Syndrome and  
430 Hypophosphatemic Rickets in the Absence of Xenotropic and Polytopic Retroviral Receptor in  
431 the Nephron. *J Am Soc Nephrol* 2017;28:1073-8.
- 432 15. Breusegem SY, Takahashi H, Giral-Arnal H, et al. Differential regulation of the renal  
433 sodium-phosphate cotransporters NaPi-IIa, NaPi-IIc, and PiT-2 in dietary potassium deficiency.  
434 *Am J Physiol Renal Physiol* 2009;297:F350-61.
- 435 16. Levi M, Gratton E, Forster IC, et al. Mechanisms of phosphate transport. *Nat Rev*  
436 *Nephrol* 2019;15:482-500.
- 437 17. Farrow EG, White KE. Recent advances in renal phosphate handling. *Nat Rev Nephrol*  
438 2010;6:207-17.
- 439 18. Cai Q, Hodgson SF, Kao PC, et al. Brief report: inhibition of renal phosphate transport by  
440 a tumor product in a patient with oncogenic osteomalacia. *N Engl J Med* 1994;330:1645-9.
- 441 19. Econs MJ, Drezner MK. Tumor-induced osteomalacia--unveiling a new hormone. *N Engl*  
442 *J Med* 1994;330:1679-81.
- 443 20. Saito T, Fukumoto S. Fibroblast Growth Factor 23 (FGF23) and Disorders of Phosphate  
444 Metabolism. *Int J Pediatr Endocrinol* 2009;2009:496514.
- 445 21. Khosravi A, Cutler CM, Kelly MH, et al. Determination of the elimination half-life of  
446 fibroblast growth factor-23. *J Clin Endocrinol Metab* 2007;92:2374-7.
- 447 22. Ho BB, Bergwitz C. FGF23 signalling and physiology. *J Mol Endocrinol* 2021;66:R23-  
448 R32.
- 449 23. Ichikawa S, Gray AK, Padgett LR, et al. Genetic rescue of glycosylation-deficient Fgf23  
450 in the Galnt3 knockout mouse. *Endocrinology* 2014;155:3891-8.

- 451 24. Ritter CS, Zhang S, Delmez J, Finch JL, Slatopolsky E. Differential expression and  
452 regulation of Klotho by paricalcitol in the kidney, parathyroid, and aorta of uremic rats. *Kidney*  
453 *Int* 2015;87:1141-52.
- 454 25. Goetz R, Nakada Y, Hu MC, et al. Isolated C-terminal tail of FGF23 alleviates  
455 hypophosphatemia by inhibiting FGF23-FGFR-Klotho complex formation. *Proc Natl Acad Sci*  
456 *U S A* 2010;107:407-12.
- 457 26. Edmonston D, Wolf M. FGF23 at the crossroads of phosphate, iron economy and  
458 erythropoiesis. *Nat Rev Nephrol* 2020;16:7-19.
- 459 27. Saki F, Kassae SR, Salehifar A, Omrani GHR. Interaction between serum FGF-23 and  
460 PTH in renal phosphate excretion, a case-control study in hypoparathyroid patients. *BMC*  
461 *Nephrol* 2020;21:176.
- 462 28. Lyles KW, Burkes EJ, Jr., McNamara CR, Harrelson JM, Pickett JP, Drezner MK. The  
463 concurrence of hypoparathyroidism provides new insights to the pathophysiology of X-linked  
464 hypophosphatemic rickets. *J Clin Endocrinol Metab* 1985;60:711-7.
- 465 29. Olauson H, Lindberg K, Amin R, et al. Targeted deletion of Klotho in kidney distal  
466 tubule disrupts mineral metabolism. *J Am Soc Nephrol* 2012;23:1641-51.
- 467 30. Kuro OM. Phosphate and Klotho. *Kidney Int* 2011;79:121:S20-3.
- 468 31. Olauson H, Lindberg K, Amin R, et al. Parathyroid-specific deletion of Klotho unravels a  
469 novel calcineurin-dependent FGF23 signaling pathway that regulates PTH secretion. *PLoS Genet*  
470 2013;9:e1003975.
- 471 32. De Beur SM, Finnegan RB, Vassiliadis J, et al. Tumors associated with oncogenic  
472 osteomalacia express genes important in bone and mineral metabolism. *J Bone Miner Res*  
473 2002;17:1102-10.
- 474 33. Leow MKS, Dogra S, Ge X, et al. Paraneoplastic Secretion of Multiple Phosphatonins  
475 From a Deep Fibrous Histiocytoma Causing Oncogenic Osteomalacia. *J Clin Endocrinol Metab*  
476 2021;106:e2299-e308.
- 477 34. Bresler D, Bruder J, Mohnike K, Fraser WD, Rowe PS. Serum MEPE-ASARM-peptides  
478 are elevated in X-linked rickets (HYP): implications for phosphaturia and rickets. *J Endocrinol*  
479 2004;183:R1-9.
- 480 35. Rowe PS, Kumagai Y, Gutierrez G, et al. MEPE has the properties of an osteoblastic  
481 phosphatonin and minihibin. *Bone* 2004;34:303-19.
- 482 36. Rowe PS, Garrett IR, Schwarz PM, et al. Surface plasmon resonance (SPR) confirms that  
483 MEPE binds to PHEX via the MEPE-ASARM motif: a model for impaired mineralization in X-  
484 linked rickets (HYP). *Bone* 2005;36:33-46.
- 485 37. Yuan B, Takaiwa M, Clemens TL, et al. Aberrant Phex function in osteoblasts and  
486 osteocytes alone underlies murine X-linked hypophosphatemia. *J Clin Invest* 2008;118:722-34.
- 487 38. Berndt TJ, Bialesz B, Craig TA, et al. Secreted frizzled-related protein-4 reduces sodium-  
488 phosphate co-transporter abundance and activity in proximal tubule cells. *Pflugers Arch*  
489 2006;451:579-87.
- 490 39. Berndt T, Craig TA, Bowe AE, et al. Secreted frizzled-related protein 4 is a potent tumor-  
491 derived phosphaturic agent. *J Clin Invest* 2003;112:785-94.
- 492 40. Christov M, Koren S, Yuan Q, Baron R, Lanske B. Genetic ablation of sfrp4 in mice does  
493 not affect serum phosphate homeostasis. *Endocrinology* 2011;152:2031-6.
- 494 41. Pande S, Ritter CS, Rothstein M, et al. FGF-23 and sFRP-4 in chronic kidney disease and  
495 post-renal transplantation. *Nephron Physiol* 2006;104:p23-32.

- 496 42. Carpenter TO, Ellis BK, Insogna KL, Philbrick WM, Sterpka J, Shimkets R. Fibroblast  
497 growth factor 7: an inhibitor of phosphate transport derived from oncogenic osteomalacia-  
498 causing tumors. *J Clin Endocrinol Metab* 2005;90:1012-20.
- 499 43. Whyte MP, Zhang F, Wenkert D, Mumm S, Berndt TJ, Kumar R. Hyperphosphatemia  
500 with low FGF7 and normal FGF23 and sFRP4 levels in the circulation characterizes pediatric  
501 hypophosphatasia. *Bone* 2020;134:115300.
- 502 44. Bansal S, Khazim K, Suri R, Martin D, Werner S, Fanti P. Tumor induced osteomalacia:  
503 associated with elevated circulating levels of fibroblast growth factor-7 in addition to fibroblast  
504 growth factor-23. *Clin Nephrol* 2016;85:57-62.
- 505 45. Alizadeh Naderi AS, Reilly RF. Hereditary disorders of renal phosphate wasting. *Nat*  
506 *Rev Nephrol* 2010;6:657-65.
- 507 46. Imel EA. Congenital Conditions of Hypophosphatemia in Children. *Calcif Tissue Int*  
508 2021;108:74-90.
- 509 47. Trombetti A, Al-Daghri N, Brandi ML, et al. Interdisciplinary management of FGF23-  
510 related phosphate wasting syndromes: a Consensus Statement on the evaluation, diagnosis and  
511 care of patients with X-linked hypophosphataemia. *Nat Rev Endocrinol* 2022;18:366-84.
- 512 48. Yuan B, Feng JQ, Bowman S, et al. Hexa-D-arginine treatment increases 7B2\*PC2  
513 activity in hyp-mouse osteoblasts and rescues the HYP phenotype. *J Bone Miner Res*  
514 2013;28:56-72.
- 515 49. Marcucci G, Brandi ML. Congenital Conditions of Hypophosphatemia Expressed in  
516 Adults. *Calcif Tissue Int* 2021;108:91-103.
- 517 50. Sabbagh Y, Carpenter TO, Demay MB. Hypophosphatemia leads to rickets by impairing  
518 caspase-mediated apoptosis of hypertrophic chondrocytes. *Proc Natl Acad Sci U S A*  
519 2005;102:9637-42.
- 520 51. Murali SK, Andrukhova O, Clinkenbeard EL, White KE, Erben RG. Excessive  
521 Osteocytic Fgf23 Secretion Contributes to Pyrophosphate Accumulation and Mineralization  
522 Defect in Hyp Mice. *PLoS Biol* 2016;14:e1002427.
- 523 52. Woeckel VJ, Alves RD, Swagemakers SM, et al. 1Alpha,25-(OH)2D3 acts in the early  
524 phase of osteoblast differentiation to enhance mineralization via accelerated production of  
525 mature matrix vesicles. *J Cell Physiol* 2010;225:593-600.
- 526 53. Clinkenbeard EL, White KE. Heritable and acquired disorders of phosphate metabolism:  
527 Etiologies involving FGF23 and current therapeutics. *Bone* 2017;102:31-9.
- 528 54. Farrow EG, Yu X, Summers LJ, et al. Iron deficiency drives an autosomal dominant  
529 hypophosphatemic rickets (ADHR) phenotype in fibroblast growth factor-23 (Fgf23) knock-in  
530 mice. *Proc Natl Acad Sci U S A* 2011;108:E1146-55.
- 531 55. Liu C, Li X, Zhao Z, et al. Iron deficiency plays essential roles in the trigger, treatment,  
532 and prognosis of autosomal dominant hypophosphatemic rickets. *Osteoporos Int* 2021;32:737-  
533 45.
- 534 56. Imel EA, Liu Z, Coffman M, Acton D, Mehta R, Econs MJ. Oral Iron Replacement  
535 Normalizes Fibroblast Growth Factor 23 in Iron-Deficient Patients With Autosomal Dominant  
536 Hypophosphatemic Rickets. *J Bone Miner Res* 2020;35:231-8.
- 537 57. Zoller H, Schaefer B, Glodny B. Iron-induced hypophosphatemia: an emerging  
538 complication. *Curr Opin Nephrol Hypertens* 2017;26:266-75.
- 539 58. Wolf M, Chertow GM, Macdougall IC, Kaper R, Krop J, Strauss W. Randomized trial of  
540 intravenous iron-induced hypophosphatemia. *JCI Insight* 2018;3.



- 541 59. Wolf M, Rubin J, Achebe M, et al. Effects of Iron Isomaltoside vs Ferric Carboxymaltose  
542 on Hypophosphatemia in Iron-Deficiency Anemia: Two Randomized Clinical Trials. *JAMA*  
543 2020;323:432-43.
- 544 60. Hoppner J, Kornak U, Sinnigen K, Rutsch F, Oheim R, Grasemann C. Autosomal  
545 recessive hypophosphatemic rickets type 2 (ARHR2) due to ENPP1-deficiency. *Bone*  
546 2021;153:116111.
- 547 61. Rutsch F, Ruf N, Vaingankar S, et al. Mutations in ENPP1 are associated with 'idiopathic'  
548 infantile arterial calcification. *Nat Genet* 2003;34:379-81.
- 549 62. Weinstein LS, Shenker A, Gejman PV, Merino MJ, Friedman E, Spiegel AM. Activating  
550 mutations of the stimulatory G protein in the McCune-Albright syndrome. *N Engl J Med*  
551 1991;325:1688-95.
- 552 63. Schwindinger WF, Francomano CA, Levine MA. Identification of a mutation in the gene  
553 encoding the alpha subunit of the stimulatory G protein of adenylyl cyclase in McCune-Albright  
554 syndrome. *Proc Natl Acad Sci U S A* 1992;89:5152-6.
- 555 64. Roszko KL, Collins MT, Boyce AM. Mosaic Effects of Growth Hormone on Fibrous  
556 Dysplasia of Bone. *N Engl J Med* 2018;379:1964-5.
- 557 65. Riminucci M, Collins MT, Fedarko NS, et al. FGF-23 in fibrous dysplasia of bone and its  
558 relationship to renal phosphate wasting. *J Clin Invest* 2003;112:683-92.
- 559 66. Folpe AL. Phosphaturic mesenchymal tumors: A review and update. *Semin Diagn Pathol*  
560 2019;36:260-8.
- 561 67. Florenzano P, Hartley IR, Jimenez M, Roszko K, Gafni RI, Collins MT. Tumor-Induced  
562 Osteomalacia. *Calcif Tissue Int* 2021;108:128-42.
- 563 68. Brandi ML, Clunie GPR, Houillier P, et al. Challenges in the management of tumor-  
564 induced osteomalacia (TIO). *Bone* 2021;152:116064.
- 565 69. Imel EA, Peacock M, Pitukcheewanont P, et al. Sensitivity of fibroblast growth factor 23  
566 measurements in tumor-induced osteomalacia. *J Clin Endocrinol Metab* 2006;91:2055-61.
- 567 70. Crotti C, Bartoli F, Coletto LA, et al. Tumor induced osteomalacia: A single center  
568 experience on 17 patients. *Bone* 2021;152:116077.
- 569 71. Zanchetta MB, Jerkovich F, Nunez S, et al. Impaired bone microarchitecture and strength  
570 in patients with tumor-induced osteomalacia. *J Bone Miner Res* 2021;36:1502-9.
- 571 72. Jiajue R, Ni X, Jin C, et al. Bone Volumetric Density, Microarchitecture, and Estimated  
572 Bone Strength in Tumor-Induced Rickets/Osteomalacia Versus X-linked Hypophosphatemia in  
573 Chinese Adolescents. *Front Endocrinol (Lausanne)* 2022;13:883981.
- 574 73. Ni X, Feng Y, Guan W, et al. Bone Impairment in a Large Cohort of Chinese Patients  
575 With Tumor-Induced Osteomalacia Assessed by HR-pQCT and TBS. *J Bone Miner Res*  
576 2022;37:454-64.
- 577 74. Cianferotti L, Delli Poggi C, Bertoldo F, et al. Persistence and recurrence in tumor-  
578 induced osteomalacia: A systematic review of the literature and results from a national  
579 survey/case series. *Endocrine* 2022;76:709-21.
- 580 75. Hidaka N, Koga M, Kimura S, et al. Clinical Challenges in Diagnosis, Tumor  
581 Localization and Treatment of Tumor-Induced Osteomalacia: Outcome of a Retrospective  
582 Surveillance. *J Bone Miner Res* 2022.
- 583 76. Ito N, Shimizu Y, Suzuki H, et al. Clinical utility of systemic venous sampling of FGF23  
584 for identifying tumours responsible for tumour-induced osteomalacia. *J Intern Med*  
585 2010;268:390-4.

- 586 77. Amanzadeh J, Reilly RF, Jr. Hypophosphatemia: an evidence-based approach to its  
587 clinical consequences and management. *Nat Clin Pract Nephrol* 2006;2:136-48.
- 588 78. Heijboer AC, Cavalier E. The Measurement and Interpretation of Fibroblast Growth  
589 Factor 23 (FGF23) Concentrations. *Calcif Tissue Int* 2022.
- 590 79. Kato H, Hidaka N, Koga M, et al. Performance evaluation of the new chemiluminescent  
591 intact FGF23 assay relative to the existing assay system. *J Bone Miner Metab* 2022;40:101-8.
- 592 80. Endo I, Fukumoto S, Ozono K, et al. Clinical usefulness of measurement of fibroblast  
593 growth factor 23 (FGF23) in hypophosphatemic patients: proposal of diagnostic criteria using  
594 FGF23 measurement. *Bone* 2008;42:1235-9.
- 595 81. Piketty ML, Brabant S, Souberbielle JC, et al. FGF23 measurement in burosumab-treated  
596 patients: an emerging treatment may induce a new analytical interference. *Clin Chem Lab Med*  
597 2020;58:e267-e9.
- 598 82. Carpenter TO, Whyte MP, Imel EA, et al. Burosumab Therapy in Children with X-  
599 Linked Hypophosphatemia. *N Engl J Med* 2018;378:1987-98.
- 600 83. Imel EA, Glorieux FH, Whyte MP, et al. Burosumab versus conventional therapy in  
601 children with X-linked hypophosphataemia: a randomised, active-controlled, open-label, phase 3  
602 trial. *Lancet* 2019;393:2416-27.
- 603 84. Whyte MP, Carpenter TO, Gottesman GS, et al. Efficacy and safety of burosumab in  
604 children aged 1-4 years with X-linked hypophosphataemia: a multicentre, open-label, phase 2  
605 trial. *Lancet Diabetes Endocrinol* 2019;7:189-99.
- 606 85. Padidela R, Whyte MP, Glorieux FH, et al. Patient-Reported Outcomes from a  
607 Randomized, Active-Controlled, Open-Label, Phase 3 Trial of Burosumab Versus Conventional  
608 Therapy in Children with X-Linked Hypophosphatemia. *Calcif Tissue Int* 2021;108:622-33.
- 609 86. Ward LM, Glorieux FH, Whyte MP, et al. Impact of Burosumab Compared with  
610 Conventional Therapy in Younger Versus Older Children with X-Linked Hypophosphatemia. *J*  
611 *Clin Endocrinol Metab* 2022.
- 612 87. Insogna KL, Briot K, Imel EA, et al. A Randomized, Double-Blind, Placebo-Controlled,  
613 Phase 3 Trial Evaluating the Efficacy of Burosumab, an Anti-FGF23 Antibody, in Adults With  
614 X-Linked Hypophosphatemia: Week 24 Primary Analysis. *J Bone Miner Res* 2018;33:1383-93.
- 615 88. Portale AA, Carpenter TO, Brandi ML, et al. Continued Beneficial Effects of Burosumab  
616 in Adults with X-Linked Hypophosphatemia: Results from a 24-Week Treatment Continuation  
617 Period After a 24-Week Double-Blind Placebo-Controlled Period. *Calcif Tissue Int*  
618 2019;105:271-84.
- 619 89. Briot K, Portale AA, Brandi ML, et al. Burosumab treatment in adults with X-linked  
620 hypophosphataemia: 96-week patient-reported outcomes and ambulatory function from a  
621 randomised phase 3 trial and open-label extension. *RMD Open* 2021;7.
- 622 90. Insogna KL, Rauch F, Kamenicky P, et al. Burosumab Improved Histomorphometric  
623 Measures of Osteomalacia in Adults with X-Linked Hypophosphatemia: A Phase 3, Single-Arm,  
624 International Trial. *J Bone Miner Res* 2019;34:2183-91.
- 625 91. Jan de Beur SM, Miller PD, Weber TJ, et al. Burosumab for the Treatment of Tumor-  
626 Induced Osteomalacia. *J Bone Miner Res* 2021;36:627-35.

627

628



## 629 **Figure and Table Captions**

630 **Figure 1.** Regulation of phosphate homeostasis by the FGF23-PTH-vitamin D axis. FGF23 and  
631 PTH reduce phosphate reabsorption in the proximal tubule. PTH also stimulates the renal  
632 production of  $1,25(\text{OH})_2\text{D}$  which subsequently increases phosphate absorption in the intestine  
633 and inhibits PTH secretion. In contrast, FGF23 and phosphate suppress the renal production of  
634  $1,25(\text{OH})_2\text{D}$ . In the parathyroid gland, phosphate stimulates secretion of PTH, whereas this  
635 secretion is inhibited by FGF23. FGF23 secretion in the bone is stimulated by PTH,  $1,25(\text{OH})_2\text{D}$ ,  
636 and phosphate. Dashed red arrows indicate inhibition, and solid green arrows indicate  
637 stimulation.

638 **Figure 2.** Intestinal phosphate absorption occurs in the small intestine via two distinct pathways:  
639 the transcellular and paracellular route. The transcellular pathway is characterized by active  
640 intestinal phosphate absorption that occurs primarily through NaPi-2b transporters in the apical  
641 membrane of enterocytes. Paracellular phosphate absorption occurs passively along  
642 concentration gradients through tight junction proteins between adjacent enterocytes. The  
643 paracellular pathway is responsible for the majority of intestinal phosphate absorption in  
644 humans. Basolateral phosphate efflux possibly occurs by facilitated diffusion through XPR1  
645 phosphate transporter.  $1,25(\text{OH})_2\text{D}$ -mediated VDR activation enhances transcellular phosphate  
646 absorption via upregulation of NaPi-2b transporters. VDR, vitamin D receptor; XPR1,  
647 xenotropic and polytropic retrovirus receptor 1.

648 **Figure 3.** The cellular mechanism of phosphate reabsorption in the proximal tubule. Most of the  
649 filtered phosphate is reabsorbed via NaPi-2a and NaPi-2c transporters in the apical membrane  
650 and depends on the basolateral  $\text{Na}^+/\text{K}^+$ -ATPase activity to maintain the  $\text{Na}^+$  gradient that drives

651 the secondary active transport process. PiT-2 transporters also contribute to the apical phosphate  
652 influx. PTH and FGF23 induce phosphaturia by reducing expression of NaPi-2a and NaPi-2c  
653 transporters. 1,25(OH)<sub>2</sub>D-mediated VDR activation increases transcellular phosphate absorption.  
654 FGF23 suppresses mitochondrial 1 $\alpha$ -hydroxylase, but induces 24-hydroxylase expression. PTH  
655 has the opposite effects. VDR, vitamin D receptor; XPR1, xenotropic and polytropic retrovirus  
656 receptor 1.

657 **Figure 4.** FGF23 production and cleavage in osteocytes and osteoblasts. FGF23 is initially  
658 produced as a 251-amino acid pre-pro-protein. After intracellular cleavage of the signal peptide,  
659 the intact FGF23 (iFGF23) is O-glycosylated by polypeptide N-acetylgalactosaminyltransferase  
660 3 (GALNT3), which prevents proteolysis and facilitates the secretion of iFGF23 as a 227-amino  
661 acid glycoprotein. Alternatively, iFGF23 can be cleaved intracellularly by proprotein  
662 convertases, yielding biologically inactive N- and C-terminal FGF23 fragments that are  
663 cosecreted with iFGF23.

664 **Figure 5.** Nomogram for derivation of tubular maximum reabsorption of phosphate per  
665 glomerular filtration rate (T<sub>mp</sub>/GFR).<sup>77</sup> C<sub>Cr</sub>, creatinine clearance; C<sub>PO<sub>4</sub></sub>, phosphate clearance;  
666 TRP, fractional tubular reabsorption of phosphate.

667 **Figure 6.** The measurement of FGF23 using immunoassays. A. The intact FGF23 immunoassay  
668 uses two monoclonal antibodies that recognize epitopes within the N-terminal and C-terminal  
669 domains of FGF23, which flank the proteolytic cleavage site, for the detection of only full-length  
670 FGF23. B. For the C-terminal FGF23 immunoassay, detecting antibodies bind to epitopes within  
671 the C-terminal domain only and this assay detects both full-length FGF23 and C-terminal FGF23  
672 fragments.

---

673 **Table 1.** Clinical conditions associated with hypophosphatemia and other useful laboratory values.

674 **Table 2.** Genetic and acquired disorders of renal phosphate handling and the associated mutations.

675 **Table 3.** Main clinical studies of burosumab in adults with XLH or TIO.

---

676

Journal Pre-proof

**Table 1.** Clinical conditions associated with hypophosphatemia and other useful laboratory values.

Clinical Conditions	S Ca	S PTH	S 25D	S 1,25D	S FGF23	U Ca	TmP/GFR	U aa
VDDR 1	↓	↑	↔	↓	↔	↓	V	V
VDDR 2	↓	↑	↔	↑	↔	↓	V	V
XLH	↔ or ↓	↔ or ↑	↔	↓ or ↔	↑	↔	↓	V
ADHR	↔ or ↓	↔ or ↑	↔	↓ or ↔	↑	↔	↓	V
TIO	↔ or ↓	↔ or ↑	↔	↓ or ↔	↑	↔	↓	V
Nutr Pi deficiency	↔ or ↓	↓	↔	↑	↔	↑	↑	↔
Nutr D Deficiency	↓	↑	↓	↓ or ↔	↔	↓	V	V
PHPT	↑	↑	↔	↑	↔	↑	↓	V
Post-transplant HPT	↑	↑	↔	↑ or ↔	↑ or ↔	V	V	V
Fanconi syndrome	↔ or ↓	↔	↔	↓ or ↔	?	V	↓	↑
Dent's disease	↔ or ↓	↔	↔	↓ or ↔	?	V	↓	↑

↔, no change; ↑, increase; ↓, decrease

**Abbreviations:** S = serum; U = urine; TMP/GFR = tubular maximum reabsorption of phosphate/ glomerular filtration rate; aa = amino acid; V = variable; PTH = parathyroid hormone; 25D = 25-hydroxyvitamin D; 1,25D = 1,25-dihydroxyvitamin D; Ca = calcium; Pi = phosphate; VDDR = vitamin D-dependent rickets; XLH = X-linked hypophosphatemia; ADHR = autosomal dominant hypophosphatemic rickets; TIO = tumor-induced osteomalacia; Nutr = nutritional; PHPT = primary hyperparathyroidism.

Journal Pre-proof

Syndrome	Gene	Mutation type	Mechanism	Serum phosphate	Serum 1,25(OH) <sub>2</sub> D	Serum PTH	Serum intact FGF23
HHRH	NaPi-2c	Loss of function	Decreased NaPi-2c expression in the proximal tubule	↓	↑	↔ or ↓	↔
XLH	PHEX	Loss of function	Increased FGF23 production in bone	↓	↔* or ↓	↔ or ↑	↑
ADHR	FGF23	Gain of function	Decreased FGF23 degradation	↓	↔* or ↓	↔ or ↑	↑
ARHR	DMP1, ENPP1, or FAM20C	Loss of function	Increased FGF23 production in bone	↓	↔* or ↓	↔ or ↑	↑
FD/MAS	GNAS1	Gain of function	Increased FGF23	↓	↔* or ↓	↔ or ↑	↑

**Table 2.** Genetic and acquired disorders of renal phosphate handling and the associated mutations.

Syndrome	Gene	Mutation type	Mechanism	Serum phosphate	Serum 1,25(OH) <sub>2</sub> D	Serum PTH	Serum intact FGF23
			production in lesions				
TIO	FN1– FGFR1 or FN1– FGF1	Gain of function	Increased FGF23 production in tumors	↓	↔* or ↓	↔ or ↑	↑
FTC	GALNT3	Loss of function	Increased FGF23 degradation	↑	↔ or ↑	↔	↓

\*Inappropriately normal; ↔, no change; ↑, increase; ↓, decrease

**Abbreviations:** ADHR, autosomal dominant hypophosphatemic rickets; ARHR, autosomal recessive hypophosphatemic rickets; DMP, dentin matrix protein; ENPP, ectonucleotide pyrophosphatase/phosphodiesterase; FAM20C, family with sequence similarity 20, member C; FD, fibrous dysplasia; FGF, fibroblast growth factor; FGFR, FGF receptor; FN, fibronectin; FTC, familial tumoral calcinosis; GALNT, polypeptide N-acetylgalactosaminyltransferase; GNAS, guanine nucleotide-binding protein G (s) subunit alpha; HHRH, hereditary hypophosphatemic rickets with hypercalciuria; MAS, McCune-Albright syndrome; PHEX, phosphate-regulating gene with homologies to endopeptidases on the X chromosome; PTH, parathyroid hormone; TIO, tumor-induced osteomalacia; XLH, X-linked hypophosphatemia.

<b>Table 3.</b> Main clinical studies of burosumab in adults with XLH or TIO.					
<b>References</b>	<b>Cohort</b>	<b>Phase</b>	<b>Study Design</b>	<b>Burosumab Dose</b>	<b>Outcomes</b>
Insogna et al. <sup>87</sup>	134 adults with XLH	3	Double-blind, placebo-controlled study (Week 24 primary analysis)	1.0 mg/kg s.c. given every 4 weeks	Therapy increased serum phosphate, enhanced fracture/pseudofracture healing, and improved some BPI-SF scores, BFI worst fatigue, and WOMAC stiffness scores.
Portale et al. <sup>88</sup>	Cohort from Insogna et al. <sup>87</sup>	3	Extension (Insogna study) – open-label period until week 48	1.0 mg/kg s.c. given every 4 weeks	- Therapy maintained serum phosphate, enhanced fracture/pseudofracture healing, and improved all BPI-SF and WOMAC scores. - Therapy also improved ambulatory function as measured with 6MWT.
Briot et al. <sup>89</sup>	Cohort from Insogna et al. <sup>87</sup>	3	Extension (Insogna study) – open-label period until week 96	1.0 mg/kg s.c. given every 4 weeks	- Therapy improved all BFI, BPI-SF, and WOMAC scores. - Ambulatory function was consistently improved with therapy.
Insogna et al. <sup>90</sup>	11 adults with XLH and completed bone biopsies at baseline and week 48	3	Open-label, single-arm study	1.0 mg/kg s.c. given every 4 weeks	Therapy increased serum phosphate, reduced pain, and improved osteomalacia as measured by bone histomorphometry.
Beur et al. <sup>91</sup>	14 adults with TIO	2	Open-label study	0.3-2.0 mg/kg s.c. given every 4 weeks	- Therapy increased serum phosphate, enhanced fracture/pseudofracture healing, and improved physical functioning with acceptable safety profile. - Therapy also improved osteomalacia as measured by bone histomorphometry.

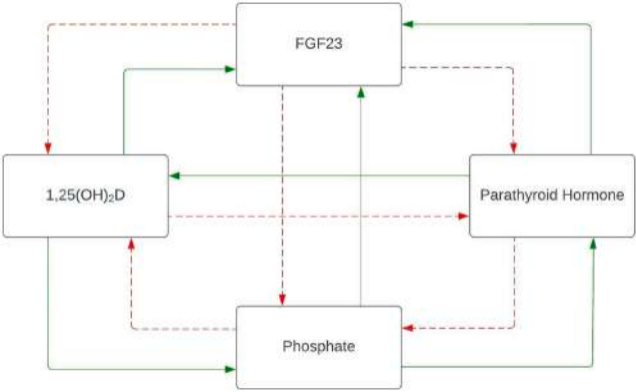


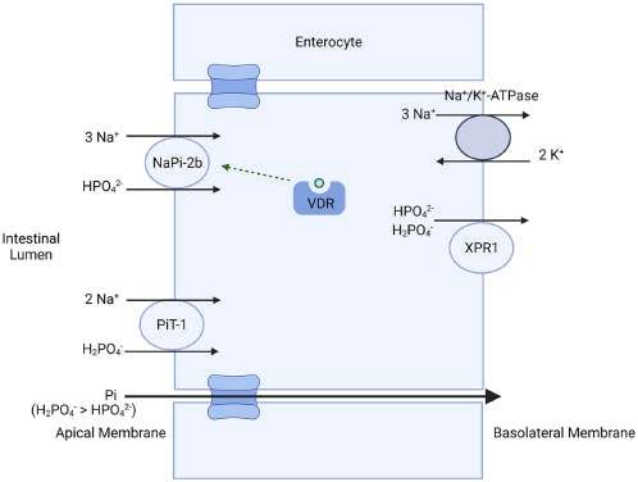
**Abbreviations:** 6MWT, 6-minute walk test; BFI, Brief Fatigue Inventory; BPI-SF, Brief Pain Inventory - Short Form; TIO, tumor-induced osteomalacia; WOMAC, Western Ontario and McMaster Osteoarthritis Index; XLH, X-linked hypophosphatemia.

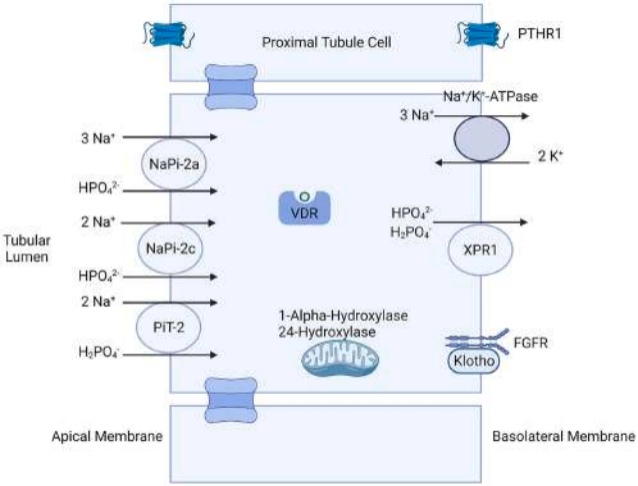
Journal Pre-proof

## Highlights

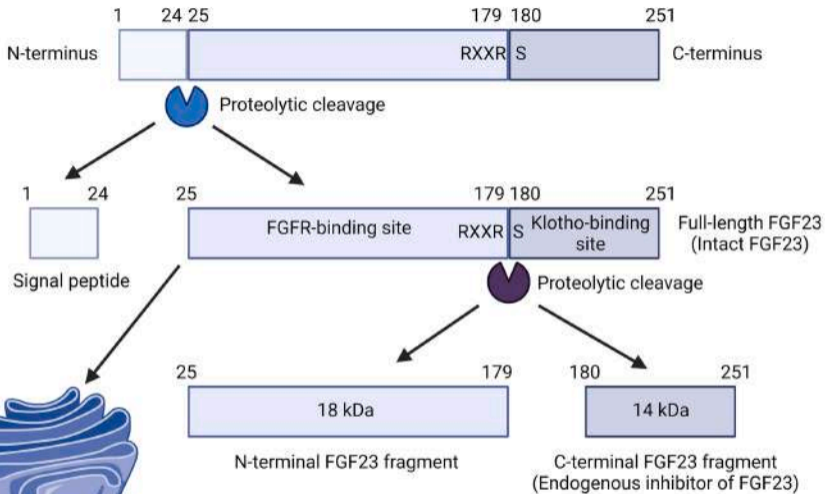
- Inorganic phosphorus is crucial for a variety of biological processes such as cell division, cellular signaling, enzyme function and skeletal integrity.
- Serum phosphate concentrations are regulated by several hormone including parathyroid hormone, 1,25-dihydroxyvitamin D and phosphatonins (especially, fibroblast growth factor 23 or FGF23).
- The absorption of phosphate in the intestine and its reabsorption in the kidney are mediated by sodium-phosphate cotransporters in the apical membrane of epithelial cells that are regulated by PTH, 1,25-dihydroxyvitamin D and FGF23.
- **Clinical Relevance:** Several hypophosphatemic disorders are mediated by abnormal concentrations of phosphate regulating hormones, especially FGF23. The etiology of these disorders can be readily diagnosed by a thorough clinical evaluation and appropriate laboratory tests. Hypophosphatemic disorders can be treated with oral phosphate, 1,25-dihydroxyvitamin D<sub>3</sub> therapy or FGF23 antibodies.



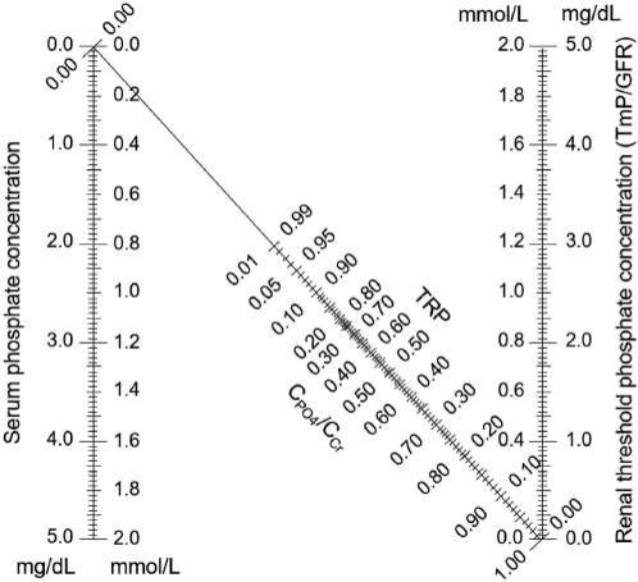




# FGF23 pre-pro-protein (251 amino acids)

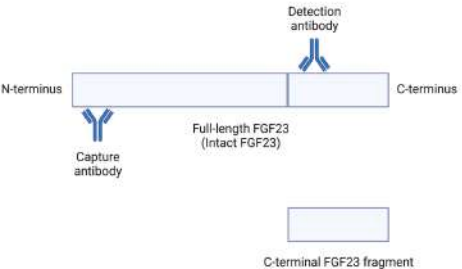


Posttranslational modification (O-Glycosylation) by GALANT3 enzyme prevents proteolysis and facilitates secretion of intact FGF23



A

## Intact FGF23 immunoassay



B

## C-terminal FGF23 immunoassay

